International Conference on Renewable Energies and Power Quality (ICREPQ'17)
Malaga (Spain), 4th to 6th April, 2017
Renewable Energy and Power Quality Journal (RE&PQJ)
ISSN 2172-038 X, No.15 April 2017

An Open-phase Fault Detection Method for Six-phase Induction Motor Drives

N. Rios-Garcia[1], M.J. Duran[1], I. Gonzalez-Prieto[1], C. Martin[2] and F. Barrero[2]

[1] Department of Electrical Engineering
E.T.S.I.I., Malaga University
29071 Malaga (Spain)
e-mail: nrg@uma.es, mjduran@uma.es, igp@uma.es

[2] Department of Electronic Engineering
E.T.S.I, Sevilla University
41092 Seville (Spain)
e-mail: cmartin15@us.es, fbarrero@us.es

Abstract. **Induction machines (IM) with multiple sets of three-phase windings are a real alternative in safety-critical applications due to their inherent redundancy and extra number of freedom degrees. These properties can be used to develop a fault-tolerant system without extra hardware. The fault detection is mandatory in the creation of a fault tolerant system. Since, the fault localization allows to adapt the control scheme of this anomalous mode of operation. Nowadays, open-phase faults (OPFs) and six-phase IMs are hot topics in the literature of fault-tolerant drives. Thus, this paper presents an open-phase fault detection method for a six-phase IM drive. The detection method is based on the vector space decomposition (VSD), taking the components of the secondary orthogonal subspace to localize the open-phase fault. The goodness of the proposed method is validated with simulation results.**

Key words: Multiphase motor drives, open-phase fault, fault detection, fault localization.

1. Introduction

Multiphase machines and drives have different advantages over standard three-phase machines [1-3]. Some of these advantages are: a certain degree of fault tolerance, a better distribution of power or a lower torque ripple. However, the most convincing one for the industry is the capability to provide fault tolerance with no extra hardware. This feature is especially valuable in safety-critical applications such as aerospace or naval drives [4-12]. In such cases, the inherent redundancy provided by multiphase systems allows the fault tolerant operation of the drive. However, the implemented control system must be able to manage the occurrence of the fault to provide a smooth post-fault operation.

The fault management in a drive can be classified in three stages: fault detection FD [13-17], fault isolation FI [18-19] and implementation of a fault tolerant control (FTC) [20-25]. The implementation of these three stages in the system is necessary to ensure a suitable operation and to protect the system in post-fault situation. The recent studies have been focused mainly in the development of FD methods and FTC strategies. Since, the fault detection is usually combined with a post-fault control [14,17]. For this reason, the requirements of an ideal detection method are the following:

- R1. A short detection time.
- R2. Capability to localize the fault.
- R3. Use of non-invasive techniques and avoid additional hardware.
- R4. Avoid complex approaches with an elevated computational cost.
- R5. Be independent of the machine parameter, control strategy and operation condition.

Even though there are some FD methods in the multiphase drives literature, none of these methods comply with the aforementioned conditions [13]. [14] proposes a detection method of dissymmetry in the stator resistance for a seven-phase IM. However, this method is dependent on the control strategy (R5 is not satisfied). R3 requirement is violated in [15-16], where additional voltage measurements are necessary to detect inter-turn short circuit. An observer-based fault detection method is presented in [17] together with a fault-tolerant finite control. This developed observer has an important computational cost and it is dependent on the machine parameters. Consequently, the R4 and R5 requirements are not complied with this method.

From the point of view of post-fault control, the open-phase fault has been the most studied fault situation regardless of the control approach [22-25]. However, there is not a detection method of this fault type that complies with the aforementioned conditions. Thus, this paper presents an open-phase localization method based on the VSD approach for a six-phase IM. The developed method uses the extra freedom degrees of multiphase machines to detect the faulty phase. These new freedom degrees are obtained due to the existence of extra orthogonal subspaces (*x-y* components in a six-phase IM). These components have the following advantages to be used as fault indices (in distributed-winding machines):

- The *x-y* components are constant (null) in healthy operation.
- The *x-y* components are not related to the torque and flux production.

Therefore, these components are independent of the drive dynamics in pre situation. This is an important requirement in the development of a detection method (R5 requirement).

The paper has been structured in the following form. Section 2 describes the topology of the studied system, the six-phase IM model, the effect of an open-phase fault and the control scheme implemented in this work. In Section 3 the proposed open-phase fault detection method is introduced. The goodness of this method is validated with simulation results in Section 4. Finally, Section 5 contains the main conclusions obtained in this paper.

2. Generalities of Six-Phase Induction Motor Drives in OPF Operation

A. Topology description

The implementation of a fault localization method must be generally combined with the utilization of a high-performance post-fault control. Therefore, it is essential that the used topology has a certain degree of fault tolerance. For this reason, the topology shown in Fig. 1, whose post-fault operation under open-phase faults has been already validated [20], has been selected in this work. This topology is formed by an asymmetrical six-phase IM fed by two voltage source converters (VSCs) that are connected to a single dc-link. The induction machine has two sets of three-phase windings ($a_1b_1c_1$ and $a_2b_2c_2$) that are spatially shifted 30° and whose neutral points are isolated. Each set of three-phase windings is connected to one three-phase VSC, as it shown in Fig. 1.

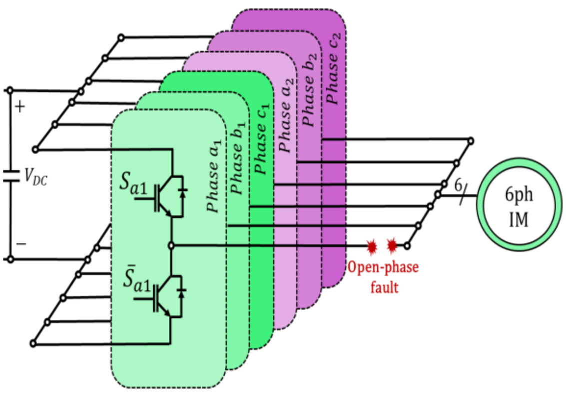

Fig.1. Scheme of a six-phase IM in OPF situation.

B. Model of the six-phase induction machine

Multiphase machine models consist of a set of differential equations. Although these equations are traditionally expressed in phase variables, they can be also expressed in different reference frames. From the point of view of the control, it is convenient to follow the VSD approach in order to control the flux and torque in a decoupled form. Firstly, the power-invariant generalized Clarke transformation is employed to express the multiphase machine model in the $\alpha\beta xy$ reference frame:

$$[T]=\frac{1}{\sqrt{3}}\begin{bmatrix} 1 & -1/2 & -1/2 & \sqrt{3}/2 & -\sqrt{3}/2 & 0 \\ 0 & \sqrt{3}/2 & -\sqrt{3}/2 & 1/2 & 1/2 & -1 \\ 1 & -1/2 & -1/2 & -\sqrt{3}/2 & \sqrt{3}/2 & 0 \\ 0 & -\sqrt{3}/2 & \sqrt{3}/2 & 1/2 & 1/2 & -1 \\ 1 & 1 & 1 & 0 & 0 & 0 \\ 0 & 0 & 0 & 1 & 1 & 1 \end{bmatrix} \quad (1)$$

$$[i_{\alpha s} i_{\beta s} i_{xs} i_{ys} i_{0+} i_{0-}]^T = [T]\cdot[i_{a1} i_{b1} i_{c1} i_{a2} i_{b2} i_{c2}]$$

If the machine has distributed windings, only the $\alpha\beta$ components will contribute to the flux and torque production. Conversely, the xy components will only produce losses. Moreover, if the machine is configured with two isolated neutrals, the 0_+0_- currents will not flow and consequently these components can be neglected. Assuming standard assumptions, the model of the asymmetrical dual three-phase induction machine in VSD variables is obtained as follows:

$$\begin{aligned}
v_{\alpha s} &= (R_s + L_s\frac{d}{dt})i_{\alpha s} + M\frac{d}{dt}i_{\alpha r} \\
v_{\beta s} &= (R_s + L_s\frac{d}{dt})i_{\beta s} + M\frac{d}{dt}i_{\beta r} \\
v_{xs} &= (R_s + L_{ls}\frac{d}{dt})i_{xs} \\
v_{ys} &= (R_s + L_{ls}\frac{d}{dt})i_{ys} \\
0 &= (R_r + L_r\frac{d}{dt})i_{\alpha r} + \omega_r L_r i_{\beta r} + M\frac{d}{dt}i_{\alpha s} + \omega_r M i_{\beta s} \\
0 &= (R_r + L_r\frac{d}{dt})i_{\beta r} - \omega_r L_r i_{\alpha r} + M\frac{d}{dt}i_{\beta s} - \omega_r M i_{\alpha s} \\
T_e &= pM(i_{\beta r} i_{\alpha s} - i_{\alpha r} i_{\beta s})
\end{aligned} \quad (2)$$

where $L_s = L_{ls} + 3L_m$, $L_r = L_{lr} + 3L_m$, $M = 3L_m$ and ω_r is the rotor electrical speed ($\omega_m = p\omega_r$, being p the pole pair number), indices s and r denote stator and rotor variables and subscripts l and m indicate leakage and magnetizing inductance, respectively.

Finally, to express the machine model in the *dqx'y'* reference frame, where d and q regulate the flux and torque production, respectively, the Park transformation is employed:

$$[D]=\begin{bmatrix}\cos\theta_s & \sin\theta_s \\ -\sin\theta_s & \cos\theta_s\end{bmatrix}$$
$$[i_{ds} i_{qs} i'_{xs} i'_{ys}]^T = [D]\cdot[i_{\alpha s} i_{\beta s} i_{xs} i_{ys}] \qquad (3)$$

C. Open-phase fault in six-phase induction motor drives

The open-phase fault can be produced in different topology components. Regarding of the damaged element when an open-phase occurs, the model described in (2) can still be used. However, in the selected topology, this type of fault implies the loss of one degree of freedom. Consequently, the VSD variables are no longer independent. The new relation between the different VSD currents will be function of the phase under fault. For example, assuming without lack of generality that the fault occurs in the phase a_1 (see Fig. 1), the following post-fault constrain appears from (1):

$$i_{xs} = -i_{\alpha s} \qquad (4)$$

However in this fault situation, there is still one extra freedom degree (the *y*-current). Its reference value can be established according to a minimum loss or minimum derating criterion [25]. For this reason, the control scheme must be modified to this post-fault situation. The necessary variations in the control scheme will depend on the selected control scheme.

D. Control scheme

The model predictive control MPC of [24] is employed in this work to regulate the multiphase drive (Fig. 2). The control schemes based in MPC allow the easy addition of constraints to the cost function. This MPC property matches with the post-fault situation previously described.

The employed control scheme has an outer speed loop that provides the *q*-current reference. The *d*-current reference is usually a constant value related with the rated flux. These reference currents are transformed into the *αβ* subspace with the inverse of Park transformation. The predictive model in Fig. 2 has three inputs: *αβxy* currents, measured speed and possible voltage vectors. The *αβxy* currents are obtained from the measured phase currents and the transformation matrix *T*. The predictive model outputs are the predicted *αβxy* currents. These currents are compared with the *αβxy* current references in the cost function. Finally, the optimal stator voltage is selected from the available voltage vectors and applied to the system.

The fault detection method interacts with the control method as follows: *i)* fault localization (B1 in the Fig. 2) and *ii)* selection of the *xy* reference currents as a function of the fault (B2 in the Fig. 2). This paper focuses only in the localization of the open-phase fault (B1). Therefore, the selection of the *xy* currents reference is out of the scope of this work. In the next section, the developed fault detection method is introduced.

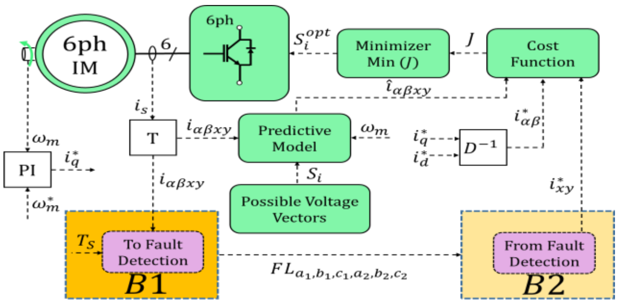

Fig. 2. MPC scheme and fault detection method.

3. Description of the proposed FD method

The proposed OPF detection and identification method is based on the study of the VSD variables, in order to overcome some disadvantages found in some of the literature methods. The objective of this section is to describe the different stages of the proposed method previously defined in the block B1 of Fig. 2.

A. Definition of the locators

From the inverse of the Clarke matrix defined in (1), it is possible to find a mathematical relation between phase currents and the *αβxy* currents of orthogonal subspaces. Adding to these equations the restriction imposed by the OPF ($i_{phase}=0$), the open-phase fault equations can be defined as:

$$\begin{aligned}
i_{a1} &= 0 \rightarrow i_{xs} = -i_{\alpha s} \\
i_{b1} &= 0 \rightarrow i_{xs} = -i_{\alpha s} + \sqrt{3}\cdot i_{\beta s} - \sqrt{3}\cdot i_{ys} \\
i_{c1} &= 0 \rightarrow i_{xs} = -i_{\alpha s} - \sqrt{3}\cdot i_{\beta s} + \sqrt{3}\cdot i_{ys} \\
i_{a2} &= 0 \rightarrow i_{xs} = i_{\alpha s} + \frac{1}{\sqrt{3}}\cdot i_{\beta s} + \frac{1}{\sqrt{3}}\cdot i_{ys} \\
i_{a2} &= 0 \rightarrow i_{xs} = i_{\alpha s} - \frac{1}{\sqrt{3}}\cdot i_{\beta s} - \frac{1}{\sqrt{3}}\cdot i_{ys} \\
i_{c2} &= 0 \rightarrow i_{ys} = -i_{\beta s}
\end{aligned} \qquad (5)$$

After that, the fault locators are defined by dividing the i_{xs} variable, or i_{ys} in case the other one does not appear, by the other side of the equalities defined in equations (5). As a result, the ratio of the locators is determined as:

$$\begin{aligned}
op_{a1} &= -\frac{i_{xs}}{i_{\alpha s}} \\
op_{b1} &= \frac{i_{xs}}{-i_{\alpha s} + \sqrt{3}\cdot i_{\beta s} - \sqrt{3}\cdot i_{ys}} \\
op_{c1} &= \frac{i_{xs}}{-i_{\alpha s} - \sqrt{3}\cdot i_{\beta s} + \sqrt{3}\cdot i_{ys}} \\
op_{a2} &= \frac{i_{xs}}{i_{\alpha s} + \frac{1}{\sqrt{3}}\cdot i_{\beta s} + \frac{1}{\sqrt{3}}\cdot i_{ys}} \\
op_{b2} &= \frac{i_{xs}}{i_{\alpha s} - \frac{1}{\sqrt{3}}\cdot i_{\beta s} - \frac{1}{\sqrt{3}}\cdot i_{ys}}
\end{aligned} \qquad (6)$$

$$op_{c2} = -\frac{i_{ys}}{i_{\beta s}}$$

These locators are close to zero when the phase is healthy. However, if an OPF occurs, the locator of that phase will have a unit value. The rest of the locators will still have a nearly null value.

B. Definition of the dead-band

Taking advantage of this behavior it is possible to introduce a dead-band to filter the response of the locators. This has to be done as the locators sometimes achieve high values when their sine waves cross zero. The definition of the dead-band is the following:

$$\begin{gathered} if \;\; 1-\delta \le op_n \le 1+\delta, \;\; then \;\; {op_n}^{db} = op_n \\ else \;\; {op_n}^{db} = 0 \end{gathered} \quad (7)$$

where δ is the width of the dead-band. This value has been chosen in accordance to the simulated results as 0.1.

C. Integration along T_m.

After that, in order to know if an OPF has occurred, the curve of the ${op_n}^{db}$ locators is integrated using a moving average defined as:

$$FL_n = \frac{1}{T_m}\int_0^{T_m} {op_n}^{db} dt \quad n \in \{a_1, b_1, c_1, a_2, b_2, c_2\} \quad (8)$$

where T_m is the period used to integrate the moving average. This parameter does not need to have be the fundamental period T_s. In fact, it can be chosen as a fraction of it in order to accelerate the OPF detection. It has to be taken into account that the lower this parameter is the higher ripple it has, but the faster detection it provides. Thus, a balance between these two characteristics will be found to choose an adequate value for T_m.

D. Definition of the threshold

Once the locators are defined (FL_n) a proper threshold must be chosen to detect the OPF. To achieve that, an equation has been developed considering the value of the six locators. The threshold thr is defined as follows:

$$thr = FL_{fp} \cdot 0.1 + FL_{hp} \quad (9)$$

where FL_{fp} is the maximum value of the faulty phase during the whole test and FL_{hp} is the highest value among the rest of the healthy phases. The 0.1 constant has been chosen looking for a fast detection and, at the same time, a reasonable margin between the threshold and the healthy phase with the highest value.

With the purpose of selecting a valid threshold, an open-phase fault has been simulated for every phase. In doing so, six different values for thr have been obtained (thr_{a1}, thr_{b1}, thr_{c1}, thr_{a2}, thr_{b2}, thr_{c2}). Thus, for the thr parameter, the highest value of all of them has been chosen so the system is able to detect an OPF in any of the six phases.

To summarize, the basic steps of the proposed method are: A) define the locators, B) use a dead-band to filter the response, C) integrate its value over T_m and D) define the threshold. As it can be seen, the procedure involves some simple mathematic operations that allow the identification of the faulty phase within milliseconds and with low computational requirements.

4. Simulation results

The objective of this section is to validate the goodness of the proposed method through simulation results. For this reason, the topology of Fig. 1, the control scheme of Fig. 2 and the developed detection method have been simulated with Matlab/Simulink. The proposed method is tested under two different operation conditions: A) open-phase faults and B) transient tests.

The IM parameters used in the simulation appear in Table I. In addition, there are other common characteristics to all the tests, as the duration of the test (1.5 s) and the instant of time when the OPF occurs (0.6 s). Finally, a step fixed of simulation of $1 \cdot 10^{-6}$s is employed in the simulation tests.

A. Open phase fault.

To run this test, in the first place the OPF is simulated in Simulink. The OFP is characterized by a null intensity once the fault has occurred. Taking this into account, at $t=0.6s$ the current in one of the six phases will be fixed to zero so it will behave as if an open-phase fault has happened.

This procedure is used to study two different situations. The first one is the OPF of the a_1 phase and the second one is the OPF of the b_2 phase. These two cases were chosen because, looking at (6), it is noticed that in the first case the only involved variable is $i_{\alpha s}$, while in the second case $i_{\alpha s}$ is implicated as well as $i_{\beta s}$, i_{xs} and i_{ys}.

The response of the system for the a_1 OPF is shown in Fig. 3. The value of the phase currents can also be seen in this figure, where since $t=0.6s$, $i_{a1}=0$. The detection time is also displayed. In order to obtain this value, a threshold was defined previously as in (9). The value chosen for thr is the most restrictive one, as it was stated before, namely $thr=0.14$. And hence, the time detection in this case is around $3.5ms$ that corresponds approximately with the

Table I. Value of the parameters of the machine

Variable	Value
R_r	2.04 Ω
R_s	4.195 Ω
L_{lr}	0.05512 H
L_{ls}	0.04245 H
L_m	0.4198 H

10% of the fundamental period. In Fig. 3, it can be seen that for all the healthy phases the locators have a close to zero value, as it was predicted in section 3.

In the case of b_2 OPF the response of the system, in Fig. 4, is as good as in the previous case. In this situation, the phase current acquiring a null value is b_2 and the detection time is around *4ms* In this figure it can also be seen that the indicators referred to the healthy phases maintain a value close to zero once the OPF has occurred.

B. Transient test.

This test has been run under two circumstances. The first one considers a variation of the load torque and the second one a variation of the i_d^*-current. These two cases have been chosen in order to prove that the *xy* components are independent of the flux and torque. In other words, the objective is to verify that the FD method is not sensitive to dynamic and flux variations. The methodology applied in Simulink to implement both conditions consists in a step block, as it implies a higher dynamic change.

The first situation considers the system response to the torque variation, shown in Fig. 5. The load torque value decreases from 8*Nm* to *0.8Nm* at *t=0.6s*. The locators stay constant and do not overpass *thr* in any case. Thus, the method developed in this paper is robust to transient dynamic tests. In Fig. 5, it can also be seen the phase currents, where the amplitude of the currents change significantly.

The second case considered is the variation of the reference i_d^*-current, shown in Fig. 6. In this case, i_d^* decreases from *1.4A* to *0.8A*. These values were chosen because of the same reason as in the torque variation. This i_d^* can be seen in Fig. 6 as well as the phase currents. In this case, the phase currents also change their values diminishing their amplitude, due to the change of the reference current. Although the i_d^* change, the locators do not vary their values. This means that the method developed is also robust to transient flux tests. In other words, the indicators do not give a false alarm in transient conditions.

In Figs. 5 and 6 it happens as defined in section 3.A. As an OPF has not occurred, the locators referred to all the phases have a null value during the whole test. Moreover, it has been proven the robustness of the method.

5. Conclusions

This work proposes a fast, robust and simple OPF detection method for six-phase IM with distributed-winding. The developed method is based on the VSD approach, specifically on the *xy*-currents. The method allows the OPF localization in a small fraction of the fundamental period. Moreover, the method is robust, since it is not sensitive to variations in the flux or torque. The use of variables involved in the control scheme avoids the need of extra hardware or complex observers. Therefore, the developed method complies with the fault detection method requirements.

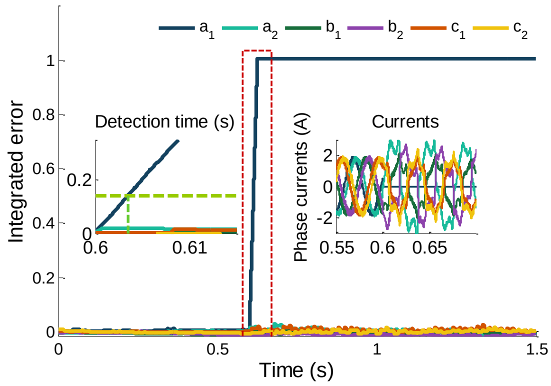

Fig. 3. Representation of the fault locators for a_1 OPF.

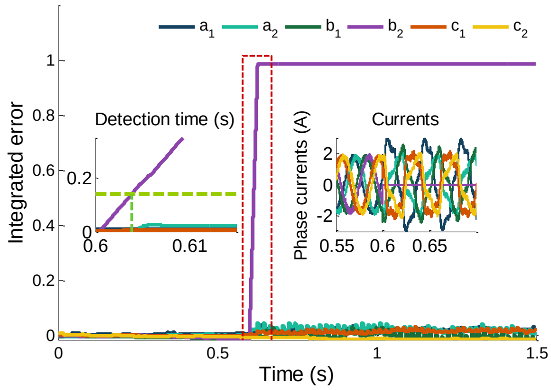

Fig. 4. Representation of the fault locators for b_2 OPF.

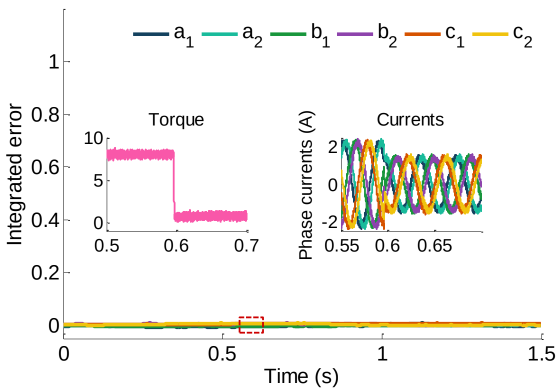

Fig. 5. Response of the system to a load torque variation.

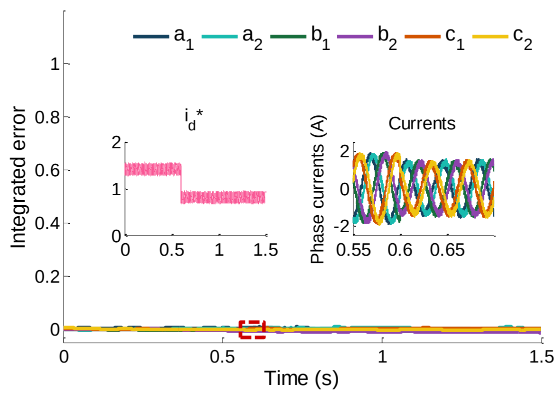

Fig. 6. Response of the system to variation of the i_d^*-current.

Acknowledgement

This work was supported by the Spanish Ministry of Science and Innovation under Project ENE2014-52536-C2–1-R.

References

[1] E. Levi, "Advances in converter control and innovative exploitation of additional degrees of freedom for multiphase machines," IEEE Trans. on Ind. Electron., vol 63, no. 1, pp. 433-448, 2016.

[2] F. Barrero and M.J. Duran, "Recent advances in the design, modeling and control of multiphase machines – Part 1," IEEE Trans. on Ind. Electron., vol 63, no. 1, pp. 449-458, 2016.

[3] M.J. Duran and F. Barrero, "Recent advances in the design, modeling and control of multiphase machines – Part 2," IEEE Trans. on Ind. Electron., vol 63, no. 1, pp. 459-468, 2016.

[4] T. McCoy and M. Bentamane, "The all-electric warship: An overview of the U.S. Navy's integrated power system development programme," in Proc. Int. Conf. ELECSHIP, Istanbul, Turkey, 1998, pp. 1–4.

[5] M. Benatmane and T. McCoy, "Development of a 19 MW PWM converter for U.S. Navy surface ships," in Proc. Int. Conf. ELECSHIP, Istanbul, Turkey, 1998, pp. 109–113.

[6] C. Hodge, S. Williamson, and A. C. Smith, "Direct drive marine propulsion motors," in Proc. Int. Conf. Electrical Machines (ICEM), Bruges, Belgium, 2002, CD-ROM, Paper 807.

[7] S. Smith, "Developments in power electronics, machines and drives," IEE Power Eng. J., vol. 16, no. 1, pp. 13–17, 2002.

[8] F. Terrien, S. Siala, and P. Noy, "Multiphase induction motor sensorless control for electric ship propulsion," in Proc. IEE PEMD Conf., Edinburgh, U.K., 2004, pp. 556–561.

[9] C. L. Ferreira and R. W. G. Bucknall, "Modelling and real-time simulation of an advanced marine full-electrical propulsion system," in Proc. IEE PEMD Conf., Edinburgh, U.K., 2004, pp. 574–579.

[10] S. D. Sudhoff, J. T. Alt, N. J. Hegner, and H. N. Robey, Jr., "Control of a 15-phase induction motor drive system," in Proc. Naval Symp. Electr.Mach., Newport, RI, 1997, pp. 69–75.

[11] S. Lu and K. Corzine, "Multilevel multi-phase propulsion drives," in Proc. IEEE ESTS, Philadelphia, PA, 2005, pp. 363–370.

[12] M. G. Simoes and P. Vieira, "A high-torque low-speed multiphase brushless machine—A perspective application for electric vehicles," IEEE Trans. Ind. Electron., vol. 49, no. 5, pp. 1154–1164, 2002.

[13] H.Henao, G.A. Capolino, M. Fernandez-Cabanas, F. Filippetti, C. Bruzzese, E. Strangas, R. Pusca, J. Estima, M. Riera-Guasp and S. Hedayati-Kia , "Trends in FaultDiagnosis for Electrical Machines: A Review of Diagnostic Techniques," IEEE Ind. Electron. Magazine, vol 8, no. 2, pp. 31-42, 2014.

[14] L. Zarri, M. Mengoni, Y. Gritli, A. Tani, F. Filippetti, G. Serra and D. Casadei, "Detection and localization of stator resistance dissymmetry based on multiple reference frame controllers in multiphase induction motor drives," IEEE Trans. Ind. Electron., vol. 60, no. 8, pp. 3506-3518, 2013.

[15] F. Immovilli, C. Bianchini, E. Lorenzani, A. Bellini and E. Fornasiero, "Evaluation of Combined Reference Frame Transformation for Interturn Fault Detection in Permanent-Magnet Multiphase Machines," IEEE Trans. Ind. Electron., vol. 62, no. 3, pp. 1912-1920, 2015.

[16] B. Sen and J. Wang, "Stator Interturn Fault Detection in Permanent-Magnet Machines Using PWM Ripple Current Measurement," IEEE Trans. Ind. Electron., vol. 63, no. 7, pp. 3148-3157, 2016.

[17] M. Salehifar, M. Moreno-Eguilaz, G. Putrus and P. Barras, "Simplified fault tolerant finite control set model predictive control of a five-phase inverter supplying BLDC motor in electric vehicle driveMehdi," Elsevier Electric Power System Research, vol. 132, pp. 56-66, 2016.

[18] S. Shao, A. J. Watson, J. C. Clare and P. W. Wheeler, "Robustness Analysis and Experimental Validation of a Fault Detection and Isolation Method for the Modular Multilevel Converter," IEEE Trans. on Power Electron., vol. 31, no. 5, pp. 3794 – 3805, 2016 .

[19] I. A. Gowaid, G. P. Adam, A. M. Massoud, S. Ahmed, D. Holliday and B. W. Williams, "Quasi Two-Level Operation of Modular Multilevel Converter for Use in a High-Power DC Transformer With DC Fault Isolation Capability," IEEE Trans. on Power Electron., vol. 30, no.1, pp. 108-123, 2015.

[20] H.S. Che, M.J. Duran, E. Levi, M. Jones, W.P. Hew and N.A. Rahim, "Post-fault operation of an asymmetrical six-phase induction machine with single and two isolated neutral points," IEEE Trans. on Power Electron., vol. 29, no. 10, pp. 5406-5416, 2014.

[21] I. Gonzalez-Prieto, M.J. Duran, F. Barrero, M. Bermudez and H. Guzman, "Impact of post-fault flux adaptation on six-phase induction motor drives with parallel converters," IEEE Trans. on Power Electron., early access, DOI: 10.1109/TPEL.2016.2533719, 2016.

[22] A. Tani, M. Mengoni, L. Zarri, G. Serra and D. Casadei, "Control of multiphase induction motors with an odd number of phases under open-circuit phase faults," IEEE Trans. Power Electron., vol. 27, no. 2, pp. 565-577, 2012.

[23] R. Kianinezhad, B. Nahid-Mobarakeh, L. Baghli, F. Betin and G.A. Capolino, "Modeling and control of six-phase symmetrical induction machine under fault condition due to open phases," IEEE Trans. Ind. Electron., vol. 55, no. 5, pp. 1996-1977, 2008.

[24] M. Bermudez, I. Gonzalez-Prieto, F. Barrero, H. Guzman, M.J. Duran, X. Kestelyn, "Open-Phase Fault-Tolerant Direct Torque Control Technique for Five-Phase Induction Motor Drives," IEEE Trans. Ind. Electron., early access, 2016.

[25] H. Guzman, M.J. Duran, F. Barrero, L. Zarri, B. Bogado, I. Gonzalez-Prieto and M.R. Arahal, "Comparative Study of Predictive and Resonant Controllers in Fault-Tolerant Five-phase Induction Motor Drives," IEEE Trans. on Ind. Electron., vol. 63, no. 1, pp. 606-617, 2016.